PHARMACOLOGY

ONC201 kills solid tumor cells by triggering an integrated stress response dependent on ATF4 activation by specific eIF2α kinases

C. Leah B. Kline,[1,2]* A. Pieter J. Van den Heuvel,[1]*† Joshua E. Allen,[1,3] Varun V. Prabhu,[1,2] David T. Dicker,[1,2] Wafik S. El-Deiry[1,2]‡

ONC201 (also called TIC10) is a small molecule that inactivates the cell proliferation– and cell survival–promoting kinases Akt and ERK and induces cell death through the proapoptotic protein TRAIL. ONC201 is currently in early-phase clinical testing for various malignancies. We found through gene expression and protein analyses that ONC201 triggered an increase in TRAIL abundance and cell death through an integrated stress response (ISR) involving the transcription factor ATF4, the transactivator CHOP, and the TRAIL receptor DR5. ATF4 was not activated in ONC201-resistant cancer cells, and in ONC201-sensitive cells, knockdown of ATF4 or CHOP partially abrogated ONC201-induced cytotoxicity and diminished the ONC201-stimulated increase in DR5 abundance. The activation of ATF4 in response to ONC201 required the kinases HRI and PKR, which phosphorylate and activate the translation initiation factor eIF2α. ONC201 rapidly triggered cell cycle arrest, which was associated with decreased abundance of cyclin D1, decreased activity of the kinase complex mTORC1, and dephosphorylation of the retinoblastoma (Rb) protein. The abundance of X-linked inhibitor of apoptosis protein (XIAP) negatively correlated with the extent of apoptosis in response to ONC201. These effects of ONC201 were independent of whether cancer cells had normal or mutant p53. Thus, ONC201 induces cell death through the coordinated induction of TRAIL by an ISR pathway.

INTRODUCTION

The discovery of the proapoptotic protein tumor necrosis factor–related apoptosis-inducing ligand (TRAIL) and its receptors in the mid- to late 1990s generated much excitement because of TRAIL's targeted apoptotic activity in cancer cells but not normal tissue (*1*). Unfortunately, the antitumor efficacy of recombinant TRAIL or TRAIL receptor antibodies [against TRAIL receptors 1 or 2 (TRAIL-R1 or TRAIL-R2), also known as death receptors 4 or 5 (DR4 or DR5), respectively] has not yet been convincingly demonstrated in clinical trials (*2*). Although the underlying mechanism for poor clinical efficacy of proapoptotic TRAIL or TRAIL receptor agonist antibodies is unclear, investigators have several theories, including increased abundance of antiapoptotic proteins such as Fas-associated death domain-like interleukin-1β–converting enzyme (FLICE) inhibitory protein (FLIP), myeloid cell leukemia-1 (Mcl-1), inhibitor of apoptosis protein-2 (IAP-2) or TRAIL decoy receptors, or decreased abundance of target proapoptotic proteins DR4 or DR5 (*2*, *3*), or insufficient receptor clustering and activation (*4*). Nevertheless, much effort has been put forth in identifying therapeutics that can be combined with TRAIL with the intent of down-regulating these inhibitory proteins or up-regulating the TRAIL receptors (*2*). On the other hand, DR5 also has ligand-independent proapoptotic capability (*5*, *6*) that can be exploited therapeutically (*7*).

We previously identified a small molecule, currently in early-phase clinical trials, called ONC201 (also known as TIC10), that not only induces TRAIL production but also increases DR5 abundance (*8*). Both TRAIL abundance and the TRAIL-DR5 interaction are required for ONC201 proapoptotic activity. Although ample evidence has been presented that TRAIL induction results from ONC201-induced activation of the transcription factor Forkhead box O3a (FOXO3a), the mechanism of DR5 up-regulation in response to ONC201 was not directly evaluated, nor were the early events that facilitate the anticancer effects of ONC201. To address these questions, we analyzed the gene expression profile of cancer cells that were treated with ONC201 at time points that precede the dual inactivation of protein kinase B (also known as Akt) and extracellular signal–regulated kinase (ERK) and the up-regulation of TRAIL abundance. Here, we report the early engagement of a stress response pathway mediated by the α subunit of eukaryotic initiation factor 2 (eIF2α) and activating transcription factor 4 (ATF4) in ONC201-treated cancer cells and detail how this pathway mediates ONC201-induced cyclin D1 down-regulation, proliferation, inhibition, and apoptosis.

RESULTS

The broad-spectrum anticancer activity of ONC201 can be attributed to its antiproliferative and proapoptotic effects

ONC201 is a novel anticancer drug that acts in part through TRAIL pathway activation. To further understand the efficacy and mechanism of action of ONC201, we treated 23 cancer cell lines, representing nine tumor types, with ONC201, determined effective concentration (EC_{50}) values (Fig. 1A, fig. S1A, and table S1), and assessed the effect of the respective EC_{50} dose on cell viability (fig. S1B). KMS18 and MM1S multiple myeloma cells were especially sensitive to ONC201, with an EC_{50} in the nanomolar range. Because ONC201 decreases the phosphorylation of Akt, ERK, and Foxo3a in various cell lines, we assessed the phosphorylation status of these proteins in a subset of the cell lines used in this study, including lymphoma and multiple myeloma cells. We confirmed the dual inhibition of the Akt and ERK pathways in many cell lines. On the other hand, there

[1]Hematology/Oncology Division and Penn State Hershey Cancer Institute, Penn State College of Medicine, Hershey, PA 17033, USA. [2]Laboratory of Translational Oncology and Experimental Cancer Therapeutics, Department of Hematology/Oncology and Molecular Therapeutics Program, Fox Chase Cancer Center, Philadelphia, PA 19111, USA. [3]Oncoceutics Inc., Hummelstown, PA 17036, USA.
*These authors contributed equally to the work.
†Present address: Vironika LLC, Philadelphia, PA 19104, USA.
‡Corresponding author. E-mail: wafik.eldeiry@fccc.edu

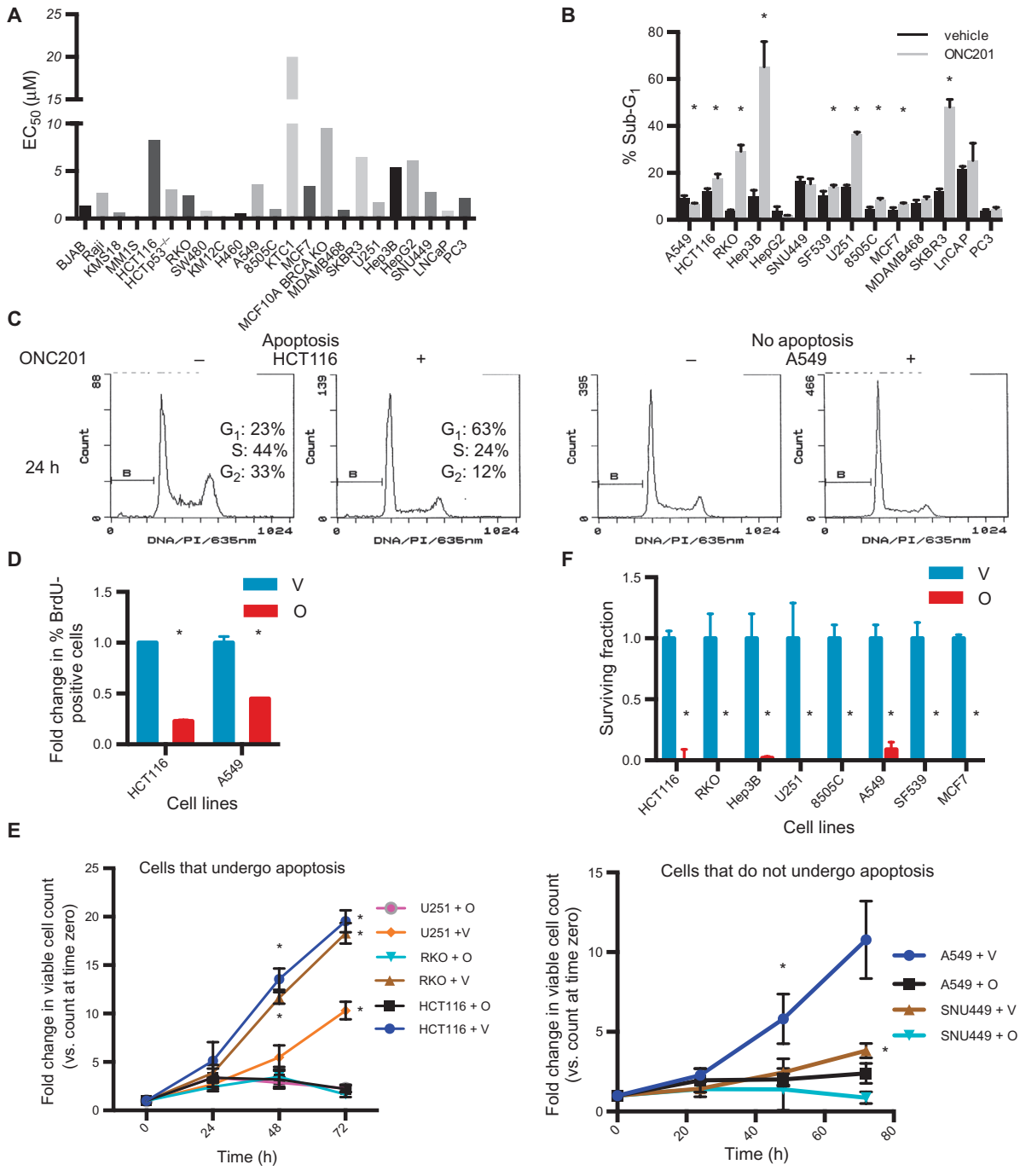

Fig. 1. ONC201's broad-spectrum activity can be attributed to its antiproliferative and proapoptotic effects. (**A**) The EC_{50} of ONC201 was assessed by CellTiter-Glo (CTG) assay in 23 cell lines treated with ONC201 for 72 hours. (**B**) Apoptosis measured by sub-G_1 analysis in cells treated with ONC201 for 72 hours. (**C**) Cell cycle profile analyses in HCT116 and A549 cells treated with ONC201 for 24 hours (H). Data are representative of two biological replicates. PI, propidium iodide. (**D**) BrdU incorporation assays in HCT116 and A549 cells treated with ONC201 for 48 hours. V, vehicle; O, ONC201. (**E**) Viable cell counts assessed by trypan blue exclusion in cells treated with ONC201 for up to 72 hours. *$P < 0.05$, Student's *t* test with Holm-Sidak correction. (**F**) Proliferative capacity of cells after 72 hours in the presence of ONC201, assessed by clonogenic assays. Bars that are not visible indicate a proliferative fraction of 0. The concentrations of ONC201 used for each cell line are listed in table S1. Data in (A), (B), (D), (E), and (F) are means ± SEM from three biological replicates.

are several cell types in which Akt and ERK phosphorylation was not decreased under the conditions used in the study (fig. S1C). We found that ONC201 not only induced apoptosis in many cell lines as measured by sub-G_1 fraction and caspase activation (Fig. 1B and fig. S1, D to F) but also induced cell cycle arrest in the cell lines tested as early as 24 hours after ONC201 treatment (Fig. 1C), before apoptosis was observed (fig. S1,

E and F). In addition, ONC201 impeded cell cycle progression regardless of whether cancer cells also underwent apoptosis in response to the drug or harbored a mutant p53 protein (Fig. 1C and fig. S1G). Bromodeoxyuridine (BrdU) labeling experiments confirmed that cell proliferation was inhibited by ONC201 (Fig. 1D). The early cell cycle arrest in response to ONC201 treatment caused a significant decrease in the number of viable cells within 48 hours (Fig. 1E), even in cells that did not undergo apoptosis (fig. S1, D to F). Moreover, ONC201 slowed down the increase in cell number even of cells that did not eventually succumb to apoptosis. This could explain, at least in part, how ONC201 exhibited broad-spectrum and potent anticancer effects, as indicated by the near-complete absence of colony formation in the clonogenic assays (Fig. 1F).

The anticancer effects of ONC201 are dependent on its engagement of the ATF4 pathway

The observation that ONC201 exerted anticancer effects, even without eventually inducing apoptosis, suggested that ONC201 perturbs pathways in addition to those previously reported (*8*). To study the possible pathways regulated by ONC201, we assessed gene expression profiles in HCT116 colon cancer cells treated with ONC201 for 18 and 48 hours and in RKO colon cancer cells treated for 48 hours (data files S1 to S7). Pathway analyses of microarray results suggested that ONC201 engaged the ATF4 pathway: many of the genes that showed increased expression with ONC201 are regulated by ATF4 (*9*) and have binding sites for ATF4 and the protein encoded by the ATF4 transcriptional target gene *CCAAT/enhancer binding*

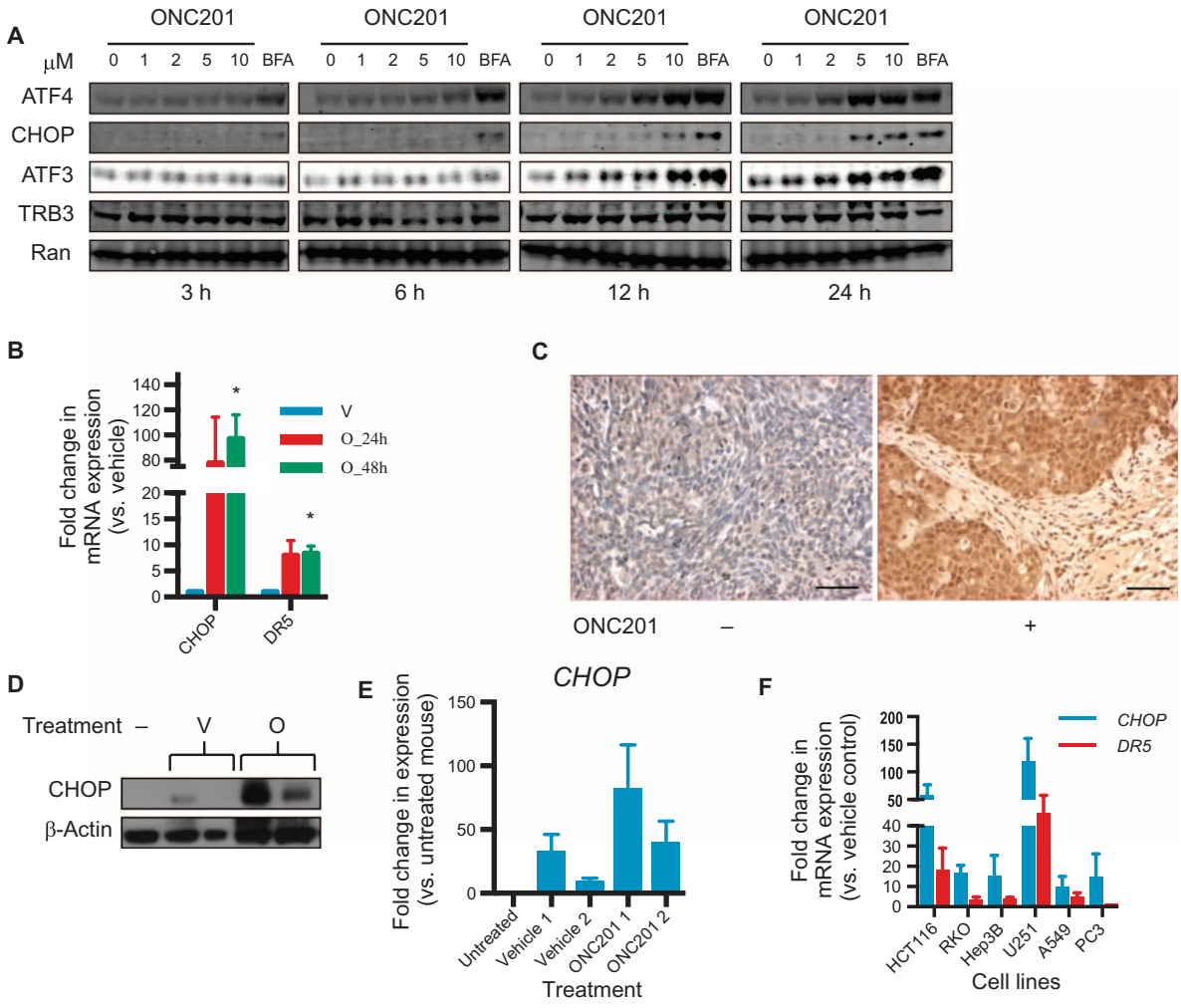

Fig. 2. ONC201 activates the ISR. (**A**) Western blotting analysis for ATF4, CHOP, ATF3, and TRB3 on lysates from HCT116 cells cultured with ONC201 (0 to 10 μM) for 3 to 24 hours. BFA (an ER stressor) served as a positive control. Blots are representative of two experiments. (**B**) Quantitative reverse transcription polymerase chain reaction (qRT-PCR) for the expression of *CHOP* and *DR5* relative to *GAPDH* in HCT116 cells treated with ONC201 (10 μM) or vehicle for 24 or 48 hours. (**C**) Immunohistochemical analysis for CHOP in HCT116-derived subcutaneous xenografts from mice that received either vehicle (–) or ONC201 (+; 25 mg/kg). Results are representative of tissues from two vehicle-treated mice and six mice intraperitoneally or intravenously injected with ONC201 (three mice each). Scale bars, 10 μm. (**D**) Western blotting analysis for CHOP in lysates from colorectal cancer stem cell–like cell-derived xenografts (*45*) in athymic nude mice extracted 72 hours after treatment [vehicle or ONC201 (50 mg/kg, intraperitoneally)]. Tumor lysates from untreated mice (–) served as controls. (**E**) Densitometric analyses of the bands in the Western blots in (D). (**F**) qRT-PCR for the fold change in expression of *CHOP* and *DR5* relative to *GAPDH* in different cell types cultured with ONC201 (compared to vehicle) for 72 hours. Data in (B), (E), and (F) are means ± SEM of three biological replicates. **P* < 0.05, Student's *t* test with Holm-Sidak correction, comparing ONC201-treated versus vehicle-treated cells.

protein homologous protein (*CHOP*) (*10*) (table S2). Western blotting analysis results confirmed that ONC201 treatment increased the abundance of ATF4 in a dose- and time-dependent manner (Fig. 2A) and in different cell types (fig. S2).

ATF4 promoted apoptosis, in part, by regulating the expression of two genes encoding the proapoptotic proteins CHOP (*11*) and DR5. *CHOP* and *DR5* expression increased in response to exposure to ONC201 in cultured HCT116 cells (Fig. 2B). We have previously reported that DR5 protein abundance is increased in tumor xenograft tissue from mice treated with ONC201 (*8*). Here, we performed immunohistochemical and Western blot analyses on colorectal cancer cell line–derived subcutaneous xenograft tumors from ONC201-treated mice, and we confirmed that ONC201 increased CHOP protein in vivo (Fig. 2, C to E). Similar to what was observed with ATF4, the increase in CHOP and DR5 abundance was also cell type–independent. Furthermore, *CHOP* and *DR5* expression was increased even in cell types that did not undergo ONC201-induced apoptosis despite exhibiting decreased cell proliferation (Fig. 2F). ATF4 has been suggested to induce cell death by promoting persistent protein synthesis, even when proteostasis has not been restored (*10*). ATF4 accomplishes this, at least in part, by increasing the expression of genes encoding protein synthesis factors, particularly aminoacyl transfer RNA (tRNA) synthetases. Our microarray analyses indicated that ONC201 induced the expression of genes encoding aminoacyl tRNA synthetases (Table 1).

We examined more closely whether ATF4 activation is critical for ONC201's anticancer effects. Cancer cells that acquired resistance to ONC201 (fig. S3, A and B) did not engage the ATF4 pathway when treated with ONC201 (Fig. 3, A and B, and table S3). Because ATF4 can be activated by pharmacological inducers of endoplasmic reticulum (ER) stress (*12*), we treated ONC201-resistant cells with ER stress inducers to verify whether the ATF4 pathway had become dysfunctional in these cells. Treatment of ONC201-resistant cells with pharmacological ER stressors brefeldin A (BFA) or bortezomib resulted in increased ATF4 and CHOP abundance (Fig. 3A and fig. S3C), indicating that the ATF pathway was intact.

Table 1. ONC201 induces the expression of mRNAs encoding aminoacyl tRNA synthetases. Fold changes in expression of mRNAs encoding aminoacyl tRNA synthetases in HCT116 and RKO cells in response to 18 and 48 hours treatment of ONC201, as determined by microarray analyses (data files S1 to S7).

Aminoacyl tRNA synthetase	Fold change versus untreated
18 hours of ONC201 incubation	
HCT116	
Cysteinyl-tRNA synthetase (CARS)	3.4
CARS	2.5
Seryl-tRNA synthetase (SARS)	2.4
Alanyl-tRNA synthetase (AARS)	2.2
Glycyl-tRNA synthetase (GARS)	2.2
Tryptophanyl-tRNA synthetase (WARS)	2
Tyrosyl-tRNA synthetase (YARS)	2
Leucyl-tRNA synthetase (LARS)	1.8
Isoleucyl-tRNA synthetase (IARS)	1.7
48 hours of ONC201 incubation	
HCT116	
GARS	2.2
RKO	
SARS	1.9
WARS	1.8
WARS	1.6

Knocking down ATF4 or CHOP impeded the ability of ONC201 to reduce cell viability (Fig. 3C). However, unlike the impact of ATF4 knockdown on the efficacy of ONC201, CHOP reduction alone did not diminish the effect of ONC201 in inducing poly(adenosine diphosphate–ribose) polymerase (PARP) cleavage (Fig. 3D). Because ATF4 and CHOP are transcriptional activators of *DR5*, knockdown of ATF4 and CHOP was performed and *DR5* expression was assessed. The reduction in ATF4 or CHOP amounts was sufficient to ablate ONC201-induced *DR5* (Fig. 3E).

ATF4 may also play a role in the ONC201-induced inactivation of Akt, through its transcriptional target, *tribbles-like protein 3* (*TRB3*) (*13*). TRB3 inhibits the kinase activity of Akt (*14*) and regulates mitogen-activated protein kinase (MAPK) family members (*15*). Knocking down TRB3 by small interfering RNA (siRNA) abrogated ONC201-induced Akt inactivation (Fig. 3F). TRB3, therefore, could provide a link between early engagement of the integrated stress response (ISR) and late suppression of the Akt pathway in ONC201-treated cells.

The ATF4 pathway is engaged as part of the ISR to enable cells to survive conditions that threaten proteostasis, such as nutrient starvation and accumulation of misfolded proteins (a condition that causes ER stress) (*12*). ISR engagement acutely suspends protein synthesis to prevent further ER stress, and the translation inhibition, in part, results in cell cycle arrest (*16*). We demonstrated that ONC201 inhibited cell cycle progression (Fig. 1, C and D, and fig. S1, A to E). The cell cycle delay caused by ONC201 correlated with a reduction in mammalian target of rapamycin complex 1 (mTORC1) activity and cyclin D1 abundance (Fig. 4 and fig. S4A) but not with a decrease in Akt and ERK phosphorylation (fig. S4B). The decrease in cyclin D1 abundance was associated with a partial reduction in the phosphorylation of retinoblastoma (Rb) protein at Ser^{795} (Fig. 4 and fig. S4A).

Given the critical role that ATF4 plays in ONC201's mechanism of cytotoxicity, we determined how ONC201 engages the ATF4 pathway. ATF4 protein abundance was generally increased after 12 hours of treatment with ONC201 (Figs. 2A and 3A and fig. S2). An increase in ATF4 protein abundance can result from the combination of increased transcription and preferential translation, the latter of which occurs because of phosphorylation of eIF2α (*17*). Indeed, ONC201 treatment induced eIF2α phosphorylation (Fig. 5A). Increased phosphorylation of eIF2α can result from the action of eIF2α kinases—general control nondepressible 2 (GCN2), heme-regulated inhibitor (HRI), RNA-dependent protein kinase (PKR) and PKR-like ER-resident protein kinase (PERK), or from the inhibition of the eIF2α phosphatase serine/threonine protein phosphatase 1 (PP1) (*18*). Phosphorylation of histone H3 (another PP1 substrate) and eIF2α was increased when cells were treated with the PP1 inhibitor calyculin A. In contrast, ONC201 induced only the phosphorylation of eIF2α, thus suggesting that ONC201 did not inhibit PP1 (fig. S5A). To identify the eIF2α kinase(s) involved in ONC201 action and to determine whether eIF2α phosphorylation was critical for the ONC201-induced increase of ATF4, we decreased the abundance of the different eIF2α kinases using siRNA. Although decreased GCN2 and PERK amounts did not abrogate the increase in ATF4, knockdown of HRI and PKR partially ablated ONC201-induced ATF4 abundance (Fig. 5B and fig. S5B). ONC201 still increased ATF4 abundance in $GCN^{-/-}$ and $PERK^{-/-}$ mouse embryonic fibroblasts (MEFs) (fig. S5C), thus providing further evidence that GCN2 and PERK may not mediate ONC201-induced eIF2α phosphorylation, at least in the cell types used in this study. Double-knockdown experiments confirmed the relevance of HRI and PKR to ATF4 activation in ONC201-treated cells: decreased ATF4 abundance was seen only in PERK- or GCN2-deficient cells when either HRI or PKR was also knocked down (Fig. 5C and fig. S5D). Next, we treated cells with plasmid constructs encoding wild-type or nonphosphorylatable (S51A) mutant eIF2α and treated them with ONC201.

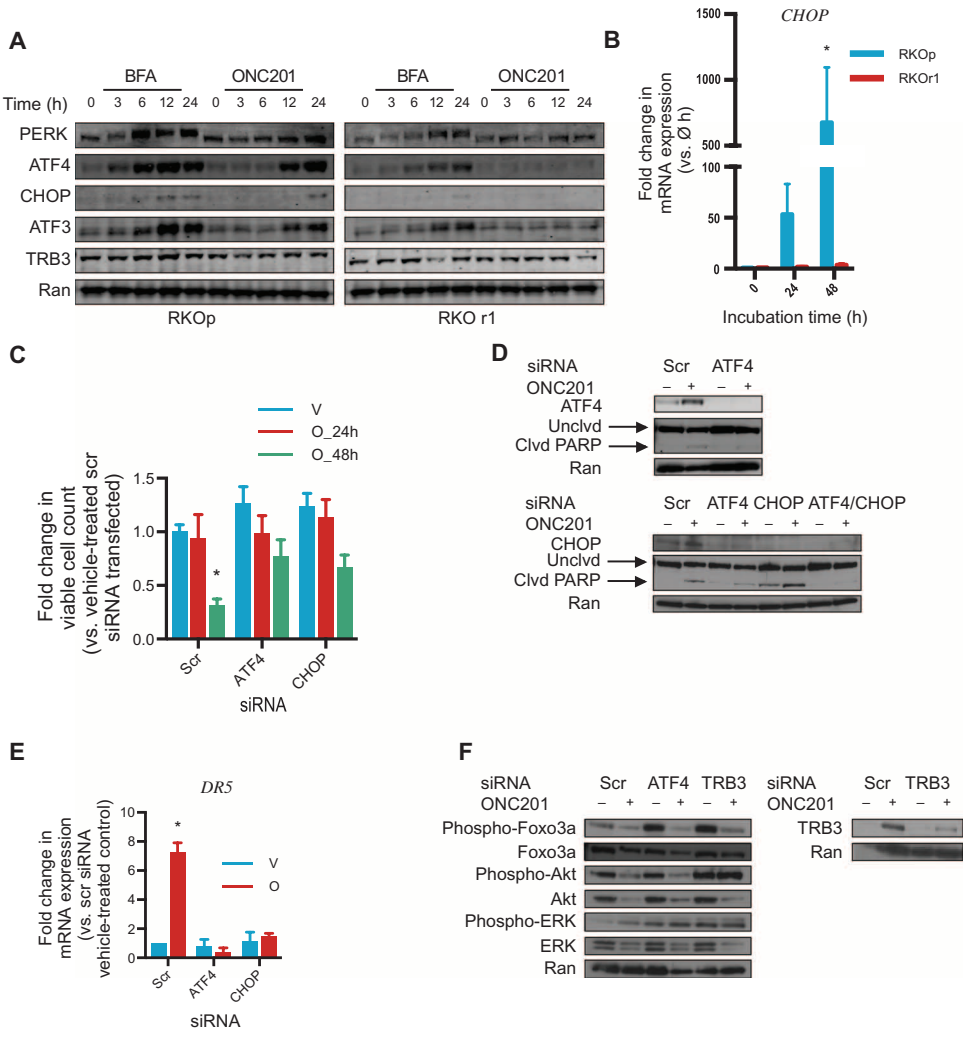

Fig. 3. ATF4 is required for ONC201-induced cytotoxicity. (**A**) Western blotting analysis for the indicated proteins in wild-type (WT) RKO (RKOp) and ONC201-resistant RKO (RKOr1) cells treated with 10 μM BFA (an ER stressor, positive control) or 5 μM ONC201. (**B**) qRT-PCR for the fold change in expression of *CHOP* relative to *GAPDH* in proteins in WT RKO and ONC201-resistant RKO cells treated with ONC201 (5 μM, 24 to 48 hours) compared with the 0 time point. (**C**) Viability of HCT116 cells assessed by trypan blue exclusion assay after ATF4 and CHOP knockdown and treatment with vehicle or ONC201 (10 μM, 24 and 48 hours). Scr, scrambled. (**D**) Western blotting analysis for ATF4, CHOP, and uncleaved (unclvd) and cleaved (clvd) PARP in HCT116 cells transfected with ATF4 or CHOP siRNA. (**E**) Quantitative PCR of *DR5* expression relative to *GAPDH* in HCT116 cells transfected with ATF4 or CHOP siRNA and subsequently treated with vehicle or ONC201 (10 μM, 48 hours). (**F**) Western blotting for the indicated proteins in HCT116 cells transfected with ATF4 or TRB3 siRNA and subsequently treated with ONC201 (10 μM, 72 hours for the left set and 48 hours for the right set). Blots in (A), (D), and (F) are representative of two experiments. Data in (B), (C), and (E) are means ± SEM of three biological replicates. *$P < 0.05$, Student's *t* test with Holm-Sidak correction.

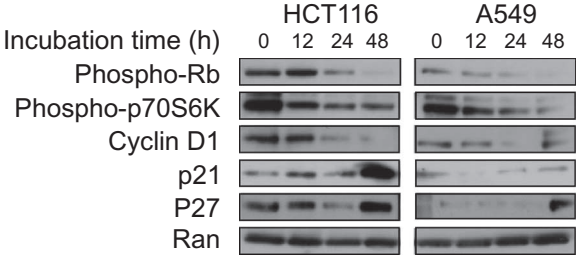

Fig. 4. ONC201 induces a decrease in cyclin D1 abundance. Western blotting analyses for the indicated proteins were performed in HCT116 or A549 cells treated with ONC201 (10 or 5 μM, respectively) for up to 48 hours. Blots are representative of two experiments.

ATF4 abundance was largely abrogated in cells expressing nonphosphorylatable mutant eIF2α (Fig. 5D). These results, therefore, demonstrated that ONC201 activated the ISR by acting through HRI and PKR to induce the phosphorylation of eIF2α and up-regulate ATF4. ONC201, however, did not appear to increase PKR kinase activity, as indicated by an absence of a substantial increase in PKR autophosphorylation (fig. S5E).

Phosphorylation of eIF2α caused cell cycle arrest, in part by down-regulating cyclin D (*19*, *20*). Given that ONC201 down-regulated cyclin D1 (Fig. 4 and fig. S4), we determined whether HRI and PKR were involved in the ONC201-induced cyclin D1 decrease. The ONC201-induced decrease in cyclin D1 abundance was partially abrogated when PKR was knocked down, either alone or in conjunction with that of HRI (Fig. 5E). These results suggest that PKR likely plays a role in ONC201-induced decrease of cyclin D1.

XIAP abundance correlates with sensitivity to ONC201-induced apoptosis

The ability of ONC201 to not only induce apoptosis but also inhibit cell proliferation may underlie the broad-spectrum anticancer activity of ONC201. The amount of X-linked inhibitor of apoptosis protein (XIAP) can prevent apoptosis in response to TRAIL induction (*21*, *22*). Here, XIAP abundance appeared to correlate with the apoptotic response of cancer cells to ONC201. In cells that undergo ONC201-induced apoptosis, XIAP amount was reduced after treatment with ONC201. In contrast, XIAP abundance persisted—although it decreased somewhat—in cells that did not undergo apoptosis (Fig. 6). By contrast, the abundance of other IAPs and B cell lymphoma 2 (Bcl-2) family members was decreased by ONC201 in different cell types

regardless of whether or not they underwent ONC201-induced apoptosis (fig. S6). Thus, ONC201-induced suppression of cellular IAP 2 (cIAP2) and anti-apoptotic Bcl-2 family members did not appear to be sufficient to push cells to undergo cell death in response to ONC201 treatment. By contrast, the extent of decrease in XIAP amounts correlated with the degree of apoptosis in response to ONC201. To determine whether altering the amount of XIAP in cells changed their susceptibility to ONC201-induced apoptosis, we overexpressed XIAP in HCT116 cells (a cell type that underwent apoptosis; Fig. 1B) and knocked down XIAP in A549 cells (a cell type that did not undergo apoptosis; Fig. 1B) (fig. S7). The extent of ONC201-induced PARP cleavage was not affected by changing XIAP abundance, indicating that XIAP by itself did not determine cell fate in response to ONC201 treatment.

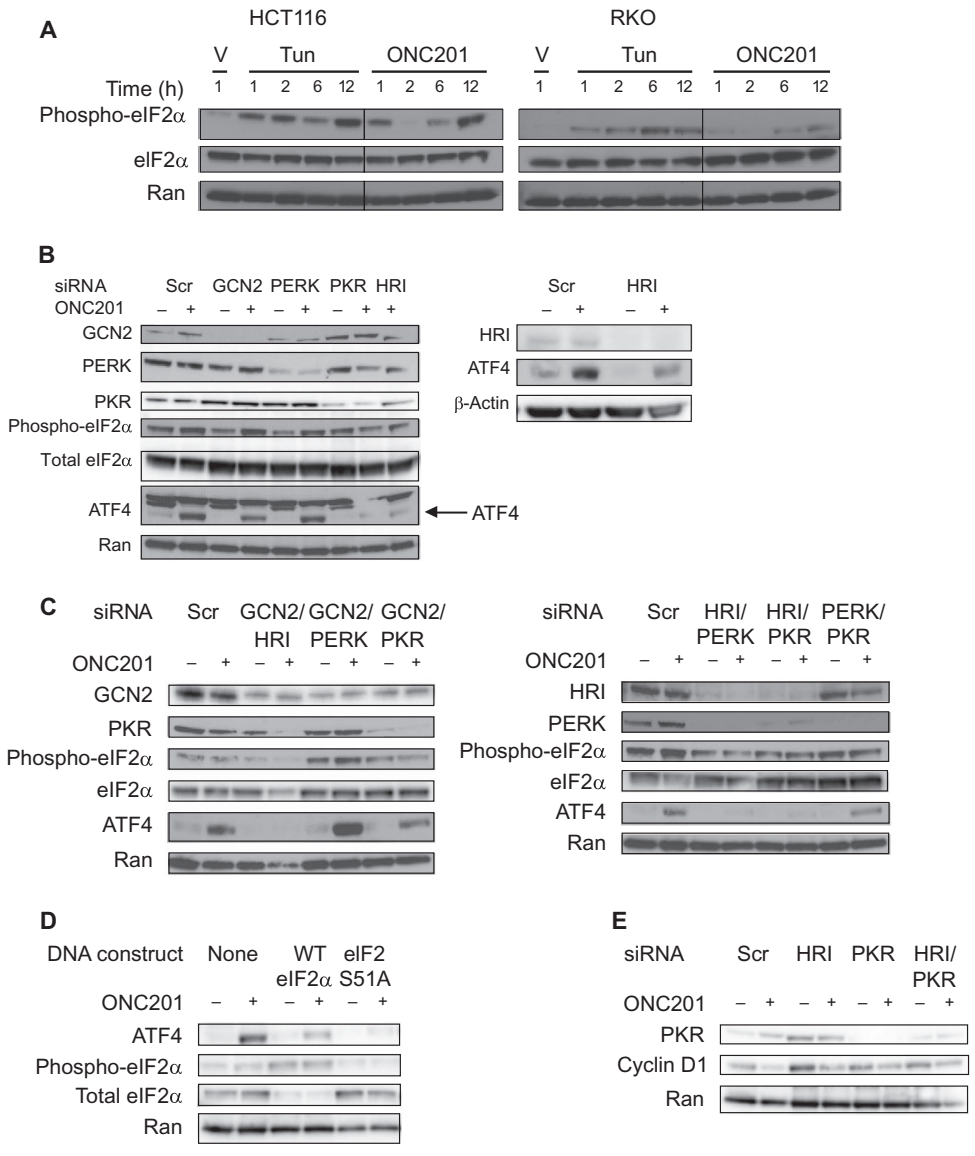

Fig. 5. ONC201 activates the ATF4 pathway through the eIF2α kinases HRI and PKR. (A) Western blotting analysis for phosphorylated and total eIF2α was performed in the indicated cell types treated with tunicamycin (Tun) or ONC201. (B to D) Western blotting analysis for the indicated proteins in lysates from HCT116 cells that were transfected with siRNA against one (B) or two eIF2α kinases (C) as indicated for 24 hours, and subsequently treated with ONC201 (10 μM) for 12 hours. (D) Western blotting analysis for indicated proteins in lysates from HCT116 cells that were transfected with plasmid constructs for WT and a nonphosphorylatable eIF2α mutant (S51A) for 48 hours and subsequently treated with ONC201 for 12 hours. (E) Western blotting analysis for cyclin D1 in HCT116 cells transfected with the indicated siRNA(s) and treated with ONC201 for 24 hours. Blots in (A) to (E) are representative of at least two independent experiments.

DISCUSSION

We uncovered a molecular mechanism that was involved in the anticancer effects of ONC201. ONC201 elicited the ISR through the eIF2α kinases HRI and PKR, resulting in activation of the eIF2α-ATF4 pathway. PKR played a role in ONC201-induced decrease in cyclin D1 abundance, and increased ATF4 abundance was required for ONC201-induced increases in DR5 abundance. Thus, we implicated the eIF2α-ATF4 pathway in the ability of ONC201 to not only induce apoptosis but also impede cell cycle progression. We confirmed the broad-spectrum anticancer activity of ONC201 and characterized the early molecular events that are critical for its efficacy.

ONC201 activated the ATF4 pathway within the first 24 hours of treatment prior to changes in Akt, ERK, and FOXO3a phosphorylation and caspase-3 activity. The ATF4 increase in ONC201-treated solid tumor cells appeared to be involved in the anticancer effects of ONC201, namely, a decrease in cell proliferation (*19*) and apoptosis that partly resulted from ATF4-mediated increases in DR5 and TRAIL abundance. Furthermore, ATF4 has been implicated in the anticancer effects of ONC201 in hematological malignancies as shown by Ishizawa *et al.* (*23*). Nevertheless, the impact of ATF4 abundance on cell viability is complex and context-dependent (*10*, *12*). Increased ATF4 abundance can be cytoprotective (*24*, *25*), antiproliferative, or cytotoxic, in part due to ATF4's potential to regulate more than 400 genes (*10*) and to interact with more than 17 proteins (*26*). It is not surprising, therefore, that the consequences of ATF4 induction by ONC201 are not identical in all cell types, as we and Ishizawa *et al.* (*23*) have shown. In HCT116 colorectal cancer cells and potentially in other solid tumor cell types, ATF4 may suppress the Akt pathway and induce apoptosis, in part through TRB3, TRAIL, and DR5. In hematologic malignancies, ATF4 and CHOP may cause cell death partly by promoting the synthesis of the proapoptotic Bcl-2 family members PUMA (*27*) and Bim (*28*), consequently activating the intrinsic apoptotic pathway.

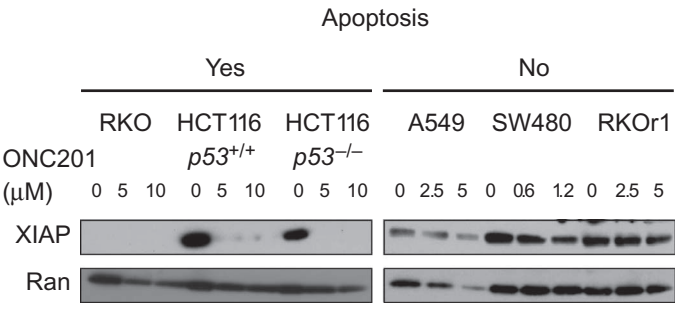

Fig. 6. The effect of ONC201 on XIAP amount correlates with fate of cells treated with ONC201. Western blotting analysis for XIAP in cells treated with the indicated concentrations of ONC201 for 72 hours. Blots are representative of at least two independent experiments.

Phosphorylation of eIF2α was critical for the ONC201-induced increase in ATF4 abundance, at least in HCT116 colorectal cancer cells, which we determined required the eIF2α kinases HRI and PKR. However, PKR, but not HRI, appeared critical for the ONC201-induced decrease in cyclin D1 abundance. Given the similarities in the kinase domains of the four eIF2α kinases (*18*), there are various contexts when at least two eIF2α kinases are involved in eIF2α phosphorylation. In fibroblasts, both PERK and GCN2 must be inhibited to counteract eIF2α phosphorylation that occurs during the unfolded protein response (UPR) (*19*). In another cell type, HT1080 cells, PERK and PKR are critical for the eIF2α-dependent decrease in cyclin D1 abundance in UPR (*20*). Their unique regulatory domains partially explain why some stresses activate specific eIF2α kinases. HRI is kept inactive by its interaction with heme and is engaged under conditions of heme depletion (*29*), but can also be activated by bortezomib (*30*, *31*) and arsenite (*32*) through poorly understood mechanisms. Small-molecule (*33*, *34*) activators of HRI have promising anticancer effects (*33*). PKR has two tandem motifs that bind double-stranded RNA molecules (*35*), which are involved in antiviral responses (*36*). However, it is also critical in other stress conditions (*37*). The versatility of PKR can be partially explained by its many potential binding partners. For instance, it activates the nuclear factor κ-light-chain enhancer of activated B cells (NF-κB) pathway by interacting with inhibitor of NF-κB kinase α (IKKα) (*38*). PKR associates with proteins involved in RNA processing, RNA binding, and protein translation, and the identity of the proteins in these complexes can be perturbed (such as in obesity) (*39*). Future studies are warranted to elucidate how ONC201 engages these two kinases. It is possible that the kinase that primarily phosphorylates eIF2α is HRI, and PKR facilitates this phosphorylation through its kinase-independent capabilities.

The relationship between eIF2α phosphorylation and the increase in ATF4 abundance in response to ONC201 treatment appeared to be cell type–specific. Whereas we found that eIF2α phosphorylation preceded the increase in ATF4 abundance in colorectal cancer cells, Ishizawa *et al.* (*23*) found that ATF4 abundance correlated with eIF2α phosphorylation in acute myeloid leukemia cell lines, but not in mantle cell lymphoma cell lines. These findings indicate that ONC201 induced ATF4 through eIF2α-dependent and eIF2α-independent mechanisms. Other pharmacological inducers of the ISR, fenretinide (a derivative of retinoic acid) and bortezomib (*40*), also engage more than one mechanism to increase ATF4 abundance. On the basis of our observations on the role of two eIF2α kinases in the ONC201-mediated increase in ATF4 abundance and Ishizawa *et al.*'s results, especially from their upstream open reading frame (uORF) reporter assay, we propose that ONC201 may enhance ATF4 abundance primarily at the translational level. Although *ATF4* mRNA translation is increased generally as a result of eIF2α phosphorylation, ATF4 abundance can be enhanced in the absence of eIF2α phosphorylation. Reductions in translation termination efficiency, such as in situations when eukaryotic release factor 3a (eRF3a) is depleted, result in increased translation of *ATF4* in a manner that is independent of eIF2α phosphorylation (*9*). Oxidative stress inhibits global protein synthesis (and presumably increases ATF4 abundance) in a manner that is dependent on phosphorylated eIF2α by inhibiting ribosomal transit (*41*).

The engagement of the ISR by ONC201 suggests some therapeutic strategies. Cell types that secrete large amounts of protein, such as the immunoglobulin-producing myeloma cells, are susceptible to ER stress and are potentially more sensitive to ISR inducers (*42*, *43*), including ONC201. This may explain at least in part the susceptibility of myeloma cells to ONC201, with EC_{50} values in the nanomolar range. The increase in CHOP abundance that occurs in cancer cells that are sensitive to ONC201 but not in resistant cells suggests that CHOP could be used as a pharmacodynamic marker for ONC201 activity. Although DR5 abundance is also increased, it may be a less suitable marker because DR5 is more ubiquitous in nature (*44*), whereas CHOP protein is generally absent under basal conditions. These results suggest that ONC201, which is currently in early-phase clinical trials in advanced solid tumors, exerts its therapeutic effects by ISR activation, which may drive the downstream dual inactivation of the Akt and ERK pathways and promote TRAIL-induced apoptosis.

MATERIALS AND METHODS

Cell culture

The human tumor cell lines were acquired from the American Type Culture Collection. HCT116 $p53^{-/-}$ cells were gifts from B. Vogelstein of Johns Hopkins University. Wild-type, $PERK^{-/-}$, and $GCN2^{-/-}$ MEFs and myeloma cells were shared by S. Kimball and N. Dolloff, respectively. The human lung, colorectal, thyroid, liver, and prostate cancer cell lines were cultured in RPMI 1640 or McCoy's 5A medium. Human breast and glioma cell lines and MEFs were maintained in Dulbecco's minimum essential medium. All basal media were supplemented with 10% fetal bovine serum (FBS) and 1% penicillin-streptomycin solution.

Viability and apoptosis assays

Viability was assayed using the CTG assay according to the manufacturer's instructions (Promega). Cells (1×10^4) were seeded in 96-well black plates and incubated for 24 hours before addition of vehicle or ONC201. To assay viability by a different method, trypan blue dye exclusion assays were performed. The cells were cultured in 24-well plates, treated with vehicle or ONC201, harvested, and stained with trypan blue. Viable cells were counted using a Cellometer cell counter.

Sub-G_1 analyses were performed to quantitate apoptosis. After treatment, floating and adherent cells were fixed in 95% ethanol and stained with propidium iodide in the presence of pancreatic ribonuclease (RNase A). Cell cycle profile and sub-G_1 analyses were performed using a Coulter-Beckman Elite Epics cytometer. To assess apoptosis by a different method, caspase-3 activity assays were performed using the Caspase-Glo 3/7 assay reagent (Promega). Cells were cultured in black 96-well plates. Parallel CTG viability assay measurements were collected and used to normalize the luminescence values collected with the Caspase-Glo 3/7 assay.

Cell proliferation was assessed by BrdU proliferation assays. Cells were incubated with 10 μM BrdU for 30 min, trypsinized, and fixed in 70% ethanol. After fixation, cells were washed and incubated with mouse anti-BrdU primary antibody (BD Biosciences) for 30 min and fluorescein isothiocyanate–conjugated anti-rabbit secondary antibody for 30 min. Cells were stained

with propidium iodide in the presence of RNase A and analyzed using a Coulter-Beckman Elite Epics cytometer.

The long-term effects of ONC201 were assessed by performing clonogenic assays. A total of 500 or 2500 cells per well were plated in six-well plates. After 24 hours of incubation, medium was replaced with that containing dimethyl sulfoxide vehicle or ONC201. After 72 hours of treatment, fresh medium without agents was added. Cells were cultured for 10 days after ONC201 removal, with replenishment of medium after 3 to 4 days. Cells were washed twice with phosphate-buffered saline (PBS), fixed, and stained with 0.25% crystal violet–methanol solution for 30 min. After washing the stain off with water, plates were allowed to dry and colonies were counted manually. Plating efficiency was calculated by dividing the number of colonies observed with the expected number of colonies. The expected number of colonies was derived by multiplying the total number of plated cells with observed percent viability (in CTG assays) after 72 hours of culture with ONC201.

In vivo study

Animal experiments were conducted in accordance with our Institutional Animal Care and Use Committee. Eight-week-old female athymic nu/nu mice (Charles River Laboratories) were inoculated with HCT116 $p53^{-/-}$ cells or sorted Aldefluor^{+} DLD1 colorectal cancer stem-like cells (*45*) in the rear flank as a 200-μl suspension of Matrigel (BD Biosciences)/PBS (1:1). Subcutaneous tumors were allowed to reach a detectable volume (~125 mm^3) before ONC201 administration. Mice that were injected with HCT116 $p53^{-/-}$ cells were treated intravenously with vehicle or ONC201 (25 mg/kg) via the tail vein, and tumor tissues were harvested after 8 hours. Mice that were injected with the colorectal cancer stem-like cells were treated intraperitoneally with either vehicle or ONC201 (50 mg/kg). Tissues were harvested after 72 hours.

Tissue analyses

Mice were humanely sacrificed by cervical dislocation under anesthesia. Tissues for Western blot analyses were minced and homogenized in lysis buffer and processed as described in the immunoblotting section below. For immunohistochemical analyses, excised tumors were fixed in 4% paraformaldehyde in PBS overnight at 4°C. Paraffin embedding and serial sectioning of slides were performed by the Penn State Hershey Histology Core Facility. Slides were dewaxed in xylene and hydrated in a decreasing gradient of ethanol. Antigen retrieval was carried out by boiling in 10 mM citric acid (pH 6.0) for 6 min. Samples were blocked with horse serum (Vector Laboratories) and incubated with primary antibody against CHOP (raised in rabbit; Santa Cruz Biotechnology) overnight at 4°C in a humidity chamber. Incubation with biotinylated secondary antibody and DAB deposition were carried out according to the manufacturer's protocol (Vector Laboratories). Samples were counterstained with hematoxylin, rinsed in distilled water, dehydrated, cleared with xylene, and mounted with Cytoseal XYL. Images were recorded on an Axioskop microscope with QCapture software (QImaging).

Isolation of ONC201-resistant clones

RKO cells were plated in six-well plates (2×10^5 cells per well) and treated with 0.5 μM ONC201 for 1 week. Cells were cultured in increasing concentrations of ONC201, up to 16 μM. Two of the wells had multiple clones and these were isolated into two separate cultures. Resistance was verified by assaying viability after ONC201 treatment and by assessing ONC201-induced surface TRAIL abundance and FOXO3a, Akt, and ERK phosphorylation.

Microarray analyses

HCT116, wild-type RKO, and ONC201-resistant RKO cells were plated in six-well plates and treated with vehicle or 5 μM ONC201. After 18 and 48 hours of treatment, RNA was isolated using the RNeasy kit (Qiagen). Gene expression analyses were performed as previously described (*8*).

Immunoblotting

Cultures were washed twice with PBS and the cells were lysed in lysis buffer [50 mM Hepes, 100 mM NaCl, 10 mM EDTA, 0.5% NP-40, 10% glycerol, supplemented with 0.0001% Tween 20, 0.1 mM phenylmethylsulfonyl fluoride, 0.1 mM $NaVO_4$, 0.5 mM NaF, leupeptin (5 μg/ml), 0.1 mM dithiothreitol]. The proteins were quantified with the Bio-Rad protein assay and loaded equally onto 4 to 12% NuPAGE SDS-polyacrylamide gels (Invitrogen). Proteins were electrophoretically transferred to polyvinylidene difluoride membranes. After blocking with 5% bovine serum albumin or 5% milk, the membranes were incubated with primary antibody overnight. Subsequently, incubation with appropriate secondary antibodies labeled with either horseradish peroxidase or near infrared (IR) dyes was performed. Signal was visualized using chemiluminescence detection or using an Odyssey Infrared Imaging System (LI-COR). The primary antibodies used in this study were as follows: antibodies against ATF4 (cat. no. 11815S), CHOP (cat. no. 2895S), DR5 (cat. no. 3696S), total eIF2α (cat. no. 9722S), BCL-2 (cat. no. 2876S), MCL-1 (cat. no. 4572S), cIAP-2 (cat. no. 3130S), BIM (cat. no. 2819S), BAX (cat. no. 5023S), phospho-Rb (S795) (cat. no. 9301S), phospho–p70 S6 kinase (cat. no. 9205S), cyclin D1 (cat. no. 2978S), phospho-FOXO3a (S253) (cat. no. 9466S), phospho-AKT (S473) (cat. no. 4051S), pan-AKT (cat. no. 4685), phospho-ERK1/2 (cat. no. 4377S), ERK (cat. no. 9102S), PKR (cat. no. 12297S), and PARP (cat. no. 9542S) (Cell Signaling); against ATF3 (sc-188), TRB3 (sc-271572), PERK (sc-377400), and HRI (sc-30143) (Santa Cruz Biotechnology); against XIAP (cat. no. 610716) and Ran (cat. no. 610341) (BD Biosciences); against phospho-eIF2α (ab32157) and FOXO3a (cat. no. ab12162) (Abcam); and against phospho-PKR (cat. no. 07-886) and p21 (cat. no. OP64-100ug) (EMD Millipore). Secondary antibodies were acquired from Pierce (cat. nos. 31430 and 31460) (horseradish peroxide–conjugated), LI-COR Biosciences (cat. no. 926-32211) (IR dye–conjugated), and Invitrogen (cat. no. A21057) (Alexa Fluor 680–conjugated).

Quantitative RT-PCR

RNA was isolated using the RNeasy kit (Qiagen) or Quick-RNA MiniPrep kit (Zymo Research) according to the manufacturer's instructions. RNA was quantitated using a NanoDrop spectrophotometer. Complementary DNA was synthesized using a SuperScript II RT kit, and real-time PCR was performed using a Quantitect SYBR Green PCR Master Mix. Relative amounts of target mRNA were quantitated using the $2^{\Delta\Delta Ct}$ method with glyceraldehyde-3-phosphate dehydrogenase (GAPDH) as internal control. At least three technical replicates per biological replicate were analyzed.

Knockdown using siRNA

Cells were plated in medium with 10% FBS but without antibiotic and incubated overnight. siRNA (a pool of three target-specific siRNAs) (40 nM final concentration; Santa Cruz Biotechnology) was transfected into cells using 9 μl of Lipofectamine RNAiMax. After 24 hours, vehicle or ONC201 was added. In the case of double knockdowns, the final concentration of each siRNA was 20 nM.

To ensure that observed effects using pooled siRNAs were not due to off-target effects, transfections were done with individual target-specific siRNAs (Sigma-Aldrich) using conditions as stated above, except that the final siRNA concentration was 13.33 nM.

Plasmid overexpression

Plasmid constructs were acquired from Addgene and amplified according to the supplier's recommendations. Plasmid DNA was isolated using the QIAprep Spin Miniprep Kit (Qiagen) according to the manufacturer's

instructions. DNA (0.5 to 1 μg) was transfected into cells using Lipofectamine 2000. Vehicle or ONC201 was added 48 hours later.

Statistics

Data are presented as means + SEM. To assess the statistical significance of the differences, unpaired Student's *t* test with Holm-Sidak correction for multiple comparisons (maximum of three comparisons were made) was performed, with $P < 0.05$ deemed statistically significant. Measurements from three biological replicates per treatment group were compared. Unless otherwise noted in the figure legend, comparisons were made against the vehicle control.

Microarray data were quantile-normalized using GenomeStudio software. Differentially expressed genes were identified with volcano plots using a fold-change threshold of 1.4 or greater and $P < 0.05$ deemed statistically significant. Multiple testing correction (Benjamini-Hochberg) was performed when the number of differentially expressed genes was greater than 1000, and the false discovery rate was set to $P < 0.05$.

SUPPLEMENTARY MATERIALS

www.sciencesignaling.org/cgi/content/full/9/415/ra18/DC1

Fig. S1. The broad-spectrum anticancer activity of ONC201 can be attributed to its antiproliferative and proapoptotic effects.

Fig. S2. ONC201 activates ATF4 and CHOP.

Fig. S3. The differential response of ONC201-sensitive and ONC201-resistant lines to ER stress inducers is correlated with ATF4 pathway activation.

Fig. S4. ONC201 induces a decrease in cyclin D1 abundance but not in Akt and ERK phosphorylation.

Fig. S5. ONC201 does not activate the eIF2α-ATF4 pathway by inhibiting the eIF2α phosphatase or by activating GCN2 or PERK.

Fig. S6. The abundance of cIAP-2 and Bcl-2 family members is similarly altered regardless of whether cells undergo apoptosis.

Fig. S7. Altering the amount of XIAP does not change ONC201's effects on PARP cleavage.

Table S1. ONC201 concentrations used according to cell type.

Table S2. Top gene expression changes induced by ONC201 in HCT116 cells.

Table S3. Top gene expression changes induced by ONC201 in RKO cells.

Data file S1. Genes in HCT116 cells with altered expression after 18 hours of ONC201 treatment.

Data file S2. Genes in HCT116 cells with altered expression after 48 hours of ONC201 treatment.

Data file S3. Additional information on the genes in data file S2.

Data file S4. Genes in HCT116 cells with altered expression after 18 or 48 hours of ONC201 treatment.

Data file S5. Genes in HCT116 cells with altered expression after 18 hours but not 48 hours of ONC201 treatment.

Data file S6. Genes in parental RKO cells with altered expression after 48 hours of ONC201 treatment.

Data file S7. Genes in ONC201-resistant RKO cells with altered expression after 48 hours of ONC201 treatment.

REFERENCES AND NOTES

1. A. Ashkenazi, R. C. Pai, S. Fong, S. Leung, D. A. Lawrence, S. A. Marsters, C. Blackie, L. Chang, A. E. McMurtrey, A. Hebert, L. DeForge, I. L. Koumenis, D. Lewis, L. Harris, J. Bussiere, H. Koeppen, Z. Shahrokh, R. H. Schwall, Safety and antitumor activity of recombinant soluble Apo2 ligand. *J. Clin. Invest.* **104**, 155–162 (1999).
2. J. Lemke, S. von Karstedt, J. Zinngrebe, H. Walczak, Getting TRAIL back on track for cancer therapy. *Cell Death Differ.* **21**, 1350–1364 (2014).
3. M. S. Merchant, J. I. Geller, K. Baird, A. J. Chou, S. Galli, A. Charles, M. Amaoko, E. H. Rhee, A. Price, L. H. Wexler, P. A. Meyers, B. C. Widemann, M. Tsokos, C. L. Mackall, Phase I trial and pharmacokinetic study of lexatumumab in pediatric patients with solid tumors. *J. Clin. Oncol.* **30**, 4141–4147 (2012).
4. K. W. Wagner, E. A. Punnoose, T. Januario, D. A. Lawrence, R. M. Pitti, K. Lancaster, D. Lee, M. von Goetz, S. F. Yee, K. Totpal, L. Huw, V. Katta, G. Cavet, S. G. Hymowitz, L. Amler, A. Ashkenazi, Death-receptor O-glycosylation controls tumor-cell sensitivity to the proapoptotic ligand Apo2L/TRAIL. *Nat. Med.* **13**, 1070–1077 (2007).
5. M. Lu, D. A. Lawrence, S. Marsters, D. Acosta-Alvear, P. Kimmig, A. S. Mendez, A. W. Paton, J. C. Paton, P. Walter, A. Ashkenazi, Opposing unfolded-protein-response signals converge on death receptor 5 to control apoptosis. *Science* **345**, 98–101 (2014).
6. S. C. Cazanave, J. L. Mott, S. F. Bronk, N. W. Werneburg, C. D. Fingas, X. W. Meng, N. Finnberg, W. S. El-Deiry, S. H. Kaufmann, G. J. Gores, Death receptor 5 signaling promotes hepatocyte lipoapoptosis. *J. Biol. Chem.* **286**, 39336–39348 (2011).
7. G. Wang, X. Wang, H. Yu, S. Wei, N. Williams, D. L. Holmes, R. Halfmann, J. Naidoo, L. Wang, L. Li, S. Chen, P. Harran, X. Lei, X. Wang, Small-molecule activation of the TRAIL receptor DR5 in human cancer cells. *Nat. Chem. Biol.* **9**, 84–89 (2013).
8. J. E. Allen, G. Krigsfeld, P. A. Mayes, L. Patel, D. T. Dicker, A. S. Patel, N. G. Dolloff, E. Messaris, K. A. Scata, W. Wang, J.-Y. Zhou, G. S. Wu, W. S. El-Deiry, Dual inactivation of Akt and ERK by TIC10 signals Foxo3a nuclear translocation, TRAIL gene induction, and potent antitumor effects. *Sci. Transl. Med.* **5**, 171ra117 (2013).
9. H. Ait Ghezala, B. Jolles, S. Salhi, K. Castrillo, W. Carpentier, N. Cagnard, A. Bruhat, P. Fafournoux, O. Jean-Jean, Translation termination efficiency modulates ATF4 response by regulating ATF4 mRNA translation at 5′ short ORFs. *Nucleic Acids Res.* **40**, 9557–9570 (2012).
10. J. Han, S. H. Back, J. Hur, Y.-H. Lin, R. Gildersleeve, J. Shan, C. L. Yuan, D. Krokowski, S. Wang, M. Hatzoglou, M. S. Kilberg, M. A. Sartor, R. J. Kaufman, ER-stress-induced transcriptional regulation increases protein synthesis leading to cell death. *Nat. Cell Biol.* **15**, 481–490 (2013).
11. H. Zinszner, M. Kuroda, X. Wang, N. Batchvarova, R. T. Lightfoot, H. Remotti, J. L. Stevens, D. Ron, CHOP is implicated in programmed cell death in response to impaired function of the endoplasmic reticulum. *Genes Dev.* **12**, 982–995 (1998).
12. H. P. Harding, Y. Zhang, H. Zeng, I. Novoa, P. D. Lu, M. Calfon, N. Sadri, C. Yun, B. Popko, R. Paules, D. F. Stojdl, J. C. Bell, T. Hettmann, J. M. Leiden, D. Ron, An integrated stress response regulates amino acid metabolism and resistance to oxidative stress. *Mol. Cell* **11**, 619–633 (2003).
13. N. Ohoka, S. Yoshii, T. Hattori, K. Onozaki, H. Hayashi, *TRB3*, a novel ER stress-inducible gene, is induced via ATF4–CHOP pathway and is involved in cell death. *EMBO J.* **24**, 1243–1255 (2005).
14. K. Du, S. Herzig, R. N. Kulkarni, M. Montminy, TRB3: A *tribbles* homolog that inhibits Akt/PKB activation by insulin in liver. *Science* **300**, 1574–1577 (2003).
15. E. Kiss-Toth, S. M. Bagstaff, H. Y. Sung, V. Jozsa, C. Dempsey, J. C. Caunt, K. M. Oxley, D. H. Wyllie, T. Polgar, M. Harte, L. A. J. O'Neill, E. E. Qwarnstrom, S. K. Dower, Human tribbles, a protein family controlling mitogen-activated protein kinase cascades. *J. Biol. Chem.* **279**, 42703–42708 (2004).
16. J. W. Brewer, L. M. Hendershot, C. J. Sherr, J. A. Diehl, Mammalian unfolded protein response inhibits cyclin D1 translation and cell-cycle progression. *Proc. Natl. Acad. Sci. U.S.A.* **96**, 8505–8510 (1999).
17. T. D. Baird, R. C. Wek, Eukaryotic initiation factor 2 phosphorylation and translational control in metabolism. *Adv. Nutr.* **3**, 307–321 (2012).
18. A. E. Koromilas, Roles of the translation initiation factor eIF2α serine 51 phosphorylation in cancer formation and treatment. *Biochim. Biophys. Acta* **1849**, 871–880 (2015).
19. R. B. Hamanaka, B. S. Bennett, S. B. Cullinan, J. A. Diehl, PERK and GCN2 contribute to eIF2α phosphorylation and cell cycle arrest after activation of the unfolded protein response pathway. *Mol. Biol. Cell* **16**, 5493–5501 (2005).
20. J. F. Raven, D. Baltzis, S. Wang, Z. Mounir, A. I. Papadakis, H. Q. Gao, A. E. Koromilas, PKR and PKR-like endoplasmic reticulum kinase induce the proteasome-dependent degradation of cyclin D1 via a mechanism requiring eukaryotic initiation factor 2α phosphorylation. *J. Biol. Chem.* **283**, 3097–3108 (2008).
21. C.-P. Ng, A. Zisman, B. Bonavida, Synergy is achieved by complementation with Apo2L/TRAIL and actinomycin D in Apo2L/TRAIL-mediated apoptosis of prostate cancer cells: Role of XIAP in resistance. *Prostate* **53**, 286–299 (2002).
22. E. H. Kim, S. U. Kim, D. Y. Shin, K. S. Choi, Roscovitine sensitizes glioma cells to TRAIL-mediated apoptosis by downregulation of survivin and XIAP. *Oncogene* **23**, 446–456 (2004).
23. J. Ishizawa, K. Kojima, D. Chachad, P. Ruvolo, V. Ruvolo, R. O. Jacamo, G. Borthakur, H. Mu, Z. Zeng, Y. Tabe, J. E. Allen, Z. Wang, W. Ma, H. C. Lee, R. Orlowski, D. D. Sarbassov, P. L. Lorenzi, X. Huang, S. S. Neelapu, T. McDonnell, R. N. Miranda, M. Wang, H. Kantarjian, M. Konopleva, R. E. Davis, M. Andreeff, ATF4 induction through an atypical integrated stress response to ONC201 induces p53-independent apoptosis in hematological malignancies. *Sci. Signal.* **9**, ra17 (2016).
24. L. R. G. Pike, D. C. Singleton, F. Buffa, O. Abramczyk, K. Phadwal, J.-L. Li, A. K. Simon, J. T. Murray, A. L. Harris, Transcriptional up-regulation of ULK1 by ATF4 contributes to cancer cell survival. *Biochem. J.* **449**, 389–400 (2013).
25. W. B'Chir, A.-C. Maurin, V. Carraro, J. Averous, C. Jousse, Y. Muranishi, L. Parry, G. Stepien, P. Fafournoux, A. Bruhat, The eIF2α/ATF4 pathway is essential for stress-induced autophagy gene expression. *Nucleic Acids Res.* **41**, 7683–7699 (2013).
26. K. Ameri, A. L. Harris, Activating transcription factor 4. *Int. J. Biochem. Cell Biol.* **40**, 14–21 (2008).
27. Z. Galehdar, P. Swan, B. Fuerth, S. M. Callaghan, D. S. Park, S. P. Cregan, Neuronal apoptosis induced by endoplasmic reticulum stress is regulated by ATF4–CHOP-mediated induction of the Bcl-2 homology 3-only member PUMA. *J. Neurosci.* **30**, 16938–16948 (2010).
28. H. Puthalakath, L. A. O'Reilly, P. Gunn, L. Lee, P. N. Kelly, N. D. Huntington, P. D. Hughes, E. M. Michalak, J. McKimm-Breschkin, N. Motoyama, T. Gotoh, S. Akira, P. Bouillet,

A. Strasser, ER stress triggers apoptosis by activating BH3-only protein Bim. *Cell* **129**, 1337–1349 (2007).
29. P. J. Chefalo, J. Oh, M. Rafie-Kolpin, B. Kan, J.-J. Chen, Heme-regulated eIF-2α kinase purifies as a hemoprotein. *Eur.J. Biochem.* **258**, 820–830 (1998).
30. M.-J. Fournier, C. Gareau, R. Mazroui, The chemotherapeutic agent bortezomib induces the formation of stress granules. *Cancer Cell Int.* **10**, 12 (2010).
31. A. Yerlikaya, S. R. Kimball, B. A. Stanley, Phosphorylation of eIF2α in response to 26S proteasome inhibition is mediated by the haem-regulated inhibitor (HRI) kinase. *Biochem. J.* **412**, 579–588 (2008).
32. E. McEwen, N. Kedersha, B. Song, D. Scheuner, N. Gilks, A. Han, J.-J. Chen, P. Anderson, R. J. Kaufman, Heme-regulated inhibitor kinase-mediated phosphorylation of eukaryotic translation initiation factor 2 inhibits translation, induces stress granule formation, and mediates survival upon arsenite exposure. *J. Biol. Chem.* **280**, 16925–16933 (2005).
33. T. Chen, D. Ozel, Y. Qiao, F. Harbinski, L. Chen, S. Denoyelle, X. He, N. Zvereva, J. G. Supko, M. Chorev, J. A. Halperin, B. H. Aktas, Chemical genetics identify eIF2α kinase heme-regulated inhibitor as an anticancer target. *Nat. Chem. Biol.* **7**, 610–616 (2011).
34. T. Chen, K. Takrouri, S. Hee-Hwang, S. Rana, R. Yefidoff-Freedman, J. Halperin, A. Natarajan, C. Morisseau, B. Hammock, M. Chorev, B. H. Aktas, Explorations of substituted urea functionality for the discovery of new activators of the heme-regulated inhibitor kinase. *J. Med. Chem.* **56**, 9457–9470 (2013).
35. S. Nanduri, B. W. Carpick, Y. Yang, B. R. G. Williams, J. Qin, Structure of the double-stranded RNA-binding domain of the protein kinase PKR reveals the molecular basis of its dsRNA-mediated activation. *EMBO J.* **17**, 5458–5465 (1998).
36. C. E. Samuel, Antiviral actions of interferon. Interferon-regulated cellular proteins and their surprisingly selective antiviral activities. *Virology* **183**, 1–11 (1991).
37. J. A. Marchal, G. J. Lopez, M. Peran, A. Comino, J. R. Delgado, J. A. García-García, V. Conde, F. M. Aranda, C. Rivas, M. Esteban, M. A. Garcia, The impact of PKR activation: From neurodegeneration to cancer. *FASEB J* **28**, 1965–1974 (2014).
38. M. Zamanian-Daryoush, T. H. Mogensen, J. A. DiDonato, B. R. G. Williams, NF-κB activation by double-stranded-RNA-activated protein kinase (PKR) is mediated through NF-κB-inducing kinase and IκB kinase. *Mol. Cell. Biol.* **20**, 1278–1290 (2000).
39. T. Nakamura, R. C. KunzC. Zhang, T. Kimura, C. L. Yuan, B. Baccaro, Y. Namiki, S. P. Gygi, G. S. Hotamisligil, A critical role for PKR complexes with TRBP in immunometabolic regulation and eIF2α phosphorylation in obesity. *Cell Rep.* **11**, 295–307 (2015).
40. J. L. Armstrong, R. Flockhart, G. J. Veal, P. E. Lovat, C. P. F. Redfern, Regulation of endoplasmic reticulum stress-induced cell death by ATF4 in neuroectodermal tumor cells. *J. Biol. Chem.* **285**, 6091–6100 (2010).
41. D. Shenton, J. B. Smirnova, J. N. Selley, K. Carroll, S. J. Hubbard, G. D. Pavitt, M. P. Ashe, C. M. Grant, Global translational responses to oxidative stress impact upon multiple levels of protein synthesis. *J. Biol. Chem.* **281**, 29011–29021 (2006).
42. E. A. Obeng, L. M. Carlson, D. M. Gutman, W. J. Harrington Jr., K. P. Lee, L. H. Boise, Proteasome inhibitors induce a terminal unfolded protein response in multiple myeloma cells. *Blood* **107**, 4907–4916 (2006).
43. A. H. Schönthal, Pharmacological targeting of endoplasmic reticulum stress signaling in cancer. *Biochem. Pharmacol.* **85**, 653–666 (2013).
44. R. A. Daniels, H. Turley, F. C. Kimberley, X. S. Liu, J. Mongkolsapaya, P. Ch'en, X. N. Xu, B. Jin, F. Pezella, G. R. Screaton, Expression of TRAIL and TRAIL receptors in normal and malignant tissues. *Cell Res.* **15**, 430–438 (2005).
45. V. V. Prabhu, J. E. Allen, D. T. Dicker, W. S. El-Deiry, Small-molecule ONC201/TIC10 targets chemotherapy-resistant colorectal cancer stem–like cells in an Akt/Foxo3a/TRAIL–dependent manner. *Cancer Res.* **75**, 1423–1432 (2015).

Acknowledgments: We acknowledge N. Dolloff (Medical University of South Carolina) for providing the myeloma cell lines; S. Kimball (Penn State College of Medicine) for the GCN2$^{-/-}$ and PERK$^{-/-}$ MEFs; D. Ron for the wild-type and nonphosphorylatable eIF2α plasmid constructs; R. Brucklacher of the Penn State Hershey Genome Sciences Facility for microarray analyses; S. Litwin and K. Devarajan of the Fox Chase Biostatistics and Bioinformatics Facility for input on appropriate statistical analyses of results; and W. J. Kline II for assistance in the preparation of figures for the manuscript. **Funding:** This work was supported by grants from the NIH (CA173453-02) and the American Cancer Society (to W.S.E.-D.). W.S.E.-D. is an American Cancer Society Research Professor. **Author contributions:** C.L.B.K., A.P.J.V.d.H., J.E.A., V.V.P., and W.S.E.-D. conceived the study and participated in the design, analyses, and interpretation of experiments. C.L.B.K., A.P.J.V.d.H., J.E.A., and V.V.P conducted the experiments. C.L.B.K., A.P.J.V.d.H., and J.E.A. wrote the manuscript. D.T.D. conducted flow cytometric analyses. W.S.E.-D. supervised the experiments and contributed as senior author including editing of the manuscript and responsibility for oversight and conduct of the research. **Competing interests:** J.E.A. and W.S.E.-D. hold a patent on ONC201 and are shareholders of Oncoceutics Inc. W.S.E.-D. is a co-founder of Oncoceutics Inc. Pennsylvania State University has licensed ONC201/TIC10 to Oncoceutics Inc. for clinical development. W.S.E.-D. is fully compliant with institutional disclosure requirements and conflict of interest rules. **Data and materials availability:** The microarray data have been deposited in the National Center for Biotechnology Information Gene Expression Omnibus database (GSE72865). ONC201 requires a materials transfer agreement from Oncoceutics.

Submitted 27 April 2015
Accepted 28 January 2016
Final Publication 16 February 2016
10.1126/scisignal.aac4374
Citation: C. L. B. Kline, A. P. J. Van den Heuvel, J. E. Allen, V. V. Prabhu, D. T. Dicker, W. S. El-Deiry, ONC201 kills solid tumor cells by triggering an integrated stress response dependent on ATF4 activation by specific eIF2α kinases. *Sci. Signal.* **9**, ra18 (2016).

Science Signaling

ONC201 kills solid tumor cells by triggering an integrated stress response dependent on ATF4 activation by specific eIF2 α kinases

C. Leah B. Kline, A. Pieter J. Van den Heuvel, Joshua E. Allen, Varun V. Prabhu, David T. Dicker and Wafik S. El-Deiry

Sci. Signal. **9** (415), ra18.
DOI: 10.1126/scisignal.aac4374

Stressing cancer cells to death

The anticancer drug ONC201 triggers cell death in various tumor types. A pair of papers (see also the Focus by Greer and Lipkowitz) show that ONC201 activated cell stress pathways that depended on the activation of the transcription factor ATF4. Kline *et al*. showed this stress response to ONC201 occurred in cells derived from various types of solid tumors, in which ATF4 activation led to an increase in the abundance of the proapoptotic protein TRAIL and its receptor DR5. Ishizawa *et al*. demonstrated that in acute myeloid leukemia and mantle cell lymphoma, ONC201 triggered apoptosis and inhibited mTORC1 signaling, a pathway that promotes cell growth and proliferation. The findings reveal more details about ONC201's mechanism of action, potentially enabling patient stratification and future development to improve its efficacy.